NASA/CR—2005-213850 AIAA–2003–0390

Additional Results of Ice-Accretion Scaling at SLD Conditions

David N. Anderson and Jen-Ching Tsao
Ohio Aerospace Institute, Brook Park, Ohio

August 2005

The NASA STI Program Office . . . in Profile

Since its founding, NASA has been dedicated to the advancement of aeronautics and space science. The NASA Scientific and Technical Information (STI) Program Office plays a key part in helping NASA maintain this important role.

The NASA STI Program Office is operated by Langley Research Center, the Lead Center for NASA's scientific and technical information. The NASA STI Program Office provides access to the NASA STI Database, the largest collection of aeronautical and space science STI in the world. The Program Office is also NASA's institutional mechanism for disseminating the results of its research and development activities. These results are published by NASA in the NASA STI Report Series, which includes the following report types:

- TECHNICAL PUBLICATION. Reports of completed research or a major significant phase of research that present the results of NASA programs and include extensive data or theoretical analysis. Includes compilations of significant scientific and technical data and information deemed to be of continuing reference value. NASA's counterpart of peer-reviewed formal professional papers but has less stringent limitations on manuscript length and extent of graphic presentations.

- TECHNICAL MEMORANDUM. Scientific and technical findings that are preliminary or of specialized interest, e.g., quick release reports, working papers, and bibliographies that contain minimal annotation. Does not contain extensive analysis.

- CONTRACTOR REPORT. Scientific and technical findings by NASA-sponsored contractors and grantees.

- CONFERENCE PUBLICATION. Collected papers from scientific and technical conferences, symposia, seminars, or other meetings sponsored or cosponsored by NASA.

- SPECIAL PUBLICATION. Scientific, technical, or historical information from NASA programs, projects, and missions, often concerned with subjects having substantial public interest.

- TECHNICAL TRANSLATION. English-language translations of foreign scientific and technical material pertinent to NASA's mission.

Specialized services that complement the STI Program Office's diverse offerings include creating custom thesauri, building customized databases, organizing and publishing research results . . . even providing videos.

For more information about the NASA STI Program Office, see the following:

- Access the NASA STI Program Home Page at ***http://www.sti.nasa.gov***

- E-mail your question via the Internet to help@sti.nasa.gov

- Fax your question to the NASA Access Help Desk at 301–621–0134

- Telephone the NASA Access Help Desk at 301–621–0390

- Write to:
  NASA Access Help Desk
  NASA Center for AeroSpace Information
  7121 Standard Drive
  Hanover, MD 21076

NASA/CR—2005-213850 AIAA–2003–0390

Additional Results of Ice-Accretion Scaling at SLD Conditions

David N. Anderson and Jen-Ching Tsao
Ohio Aerospace Institute, Brook Park, Ohio

Prepared for the
41st Aerospace Sciences Meeting and Exhibit
sponsored by the American Institute of Aeronautics and Astronautics
Reno, Nevada, January 6–9, 2003

Prepared under Cooperative Agreement NCC3–884

National Aeronautics and
Space Administration

Glenn Research Center

August 2005

Acknowledgments

The INTA, NASA Glenn Research Center Icing Branch and the FAA contributed to the work reported here. The Icing Research Tunnel (IRT) studies were supported under a grant from NASA to the Ohio Aerospace Institute. The authors wish to thank Jim Riley of the FAA and Tom Bond of NASA for their support of these tests and the IRT personnel for their excellent and committed technical support.

This report contains preliminary findings, subject to revision as analysis proceeds.

Available from

NASA Center for Aerospace Information
7121 Standard Drive
Hanover, MD 21076

National Technical Information Service
5285 Port Royal Road
Springfield, VA 22100

Available electronically at http://gltrs.grc.nasa.gov

Additional Results of Ice-Accretion Scaling at SLD Conditions

David N. Anderson and Jen-Ching Tsao
Ohio Aerospace Institute
Brook Park, Ohio 44142

Abstract

To determine scale velocity an additional similarity parameter is needed to supplement the Ruff scaling method. A Weber number based on water droplet *MVD* has been included in several studies because the effect of droplet splashing on ice accretion was believed to be important, particularly for SLD conditions. In the present study, ice shapes recorded at Appendix-C conditions and recent results at SLD conditions are reviewed to show that droplet diameter cannot be important to main ice shape, and for low airspeeds splashing does not appear to affect SLD ice shapes. Evidence is presented to show that while a supplementary similarity parameter probably has the form of a Weber number, it must be based on a length proportional to model size rather than *MVD*. Scaling comparisons were made between SLD reference conditions and Appendix-C scale conditions using this Weber number. Scale-to-reference model size ratios were 1:1.7 and 1:3.4. The reference tests used a 91-cm-chord NACA 0012 model with a velocity of approximately 50 m/s and an *MVD* of 160μm. Freezing fractions of 0.3, 0.4 and 0.5 were included in the study.

Nomenclature

A_c	Accumulation parameter, dimensionless
b	Relative heat factor, dimensionless
c	Airfoil chord, cm
c_p	Specific heat of air, cal/g K
$c_{p,ws}$	Specific heat of water at the surface temperature, cal/g K
d	Cylinder diameter or twice the leading-edge radius of airfoil, cm
h_c	Convective heat-transfer coefficient, cal/s m^2 K
h_G	Gas-phase mass-transfer coefficient, g/s m^2
K	Inertia parameter, dimensionless
K_0	Modified inertia parameter, dimensionless
L	Length proportional to model size, cm
LWC	Cloud liquid-water content, g/m^3
MVD	Water droplet median volume diameter, μm
n	Freezing fraction, dimensionless
P	General similarity parameter, dimensionless
p	Pressure, Nt/m^2
p_w	Vapor pressure of water in atmosphere, Nt/m^2
p_{ww}	Vapor pressure of water at the icing surface, Nt/m^2
r	Recovery factor, dimensionless
Re	Reynolds number of model, dimensionless
Re_δ	Reynolds number of water droplet, dimensionless
SLD	Super-cooled large droplet
t_f	Freezing temperature, °C
t_s	Surface temperature, °C
t	Temperature, °C
T	Absolute temperature, K
V	Air velocity, m/s
We	Weber number based on droplet size and water properties, dimensionless
We_c	Weber number based on model size and air properties, dimensionless
We_L	Weber number based on model size and water properties, dimensionless
β_0	Collection efficiency at stagnation line, dimensionless
ϕ	Droplet energy transfer parameter, °C
λ	Droplet range, m
λ_{Stokes}	Droplet range if Stokes Law applies, m
Λ_f	Latent heat of freezing, cal/g
Λ_v	Latent heat of condensation, cal/g
μ	Air viscosity, g/m s
θ	Air energy transfer parameter, °C
ρ	Air density, g/m^3
ρ_i	Ice density, g/m^3
ρ_w	Liquid water density, g/m^3
σ	Surface tension of water over air, dyne/cm
τ	Accretion time, min

Subscripts

R	Reference
S	Scale
st	static
tot	total

Introduction

Various icing scaling studies over the past 50 years (see, for example, Ruff[1]) have accepted that the most important similarity parameters affecting ice shape are the freezing fraction, n, accumulation parameter, A_c, and modified inertia parameter, K_0. The leading-edge collection efficiency, β_0, is directly dependent on K_0. For scale tests, these three parameters are matched to their respective reference values (established from the full-scale or reference conditions to be simulated). A fourth parameter, either the droplet energy transfer parameter, ϕ, or air energy transfer parameter, θ, was included in Ruff's scaling analysis. The four equations that result can then be solved for the scale temperature, *LWC*, time and *MVD*. For glaze ice accretions, an additional parameter is needed to determine scale velocity. The identification of this parameter has been the subject of ongoing studies for several years.[2,3,4] Here evidence from past studies along with some recent SLD ice shapes will be examined to identify the probable form of this parameter. Results from using this parameter in SLD-to-Appendix C scaling tests will be presented.

Scaling Equations

The basic defining equations for the similarity parameters used here followed Ruff.[1] The scaling method involved matching scale and reference values of the similarity parameters, A_c and n, with other parameters evaluated for comparison. In Ruff's method, the scale velocity was set at the user's convenience; in this study it was determined by matching a Weber number to be defined later. The equations for the remaining similarity parameters will be presented here.

The modified inertia parameter, K_0, was defined by Langmuir and Blodgett:[5]

$$K_0 = \frac{1}{8} + \frac{\lambda}{\lambda_{Stokes}}\left(K - \frac{1}{8}\right) \tag{1}$$

In equation (1), K is the inertia parameter,

$$K = \frac{\rho_w MVD^2 V}{18 d \mu} \tag{2}$$

where d is the diameter for cylindrical models or twice the leading-edge radius for airfoils. For the NACA 0012, a leading-edge radius of $0.0158c$ was used (see Abbott and von Doenhoff[6]), where c is the model chord. λ/λ_{Stokes} is the droplet range parameter, defined as the ratio of actual droplet range to that if Stokes drag law for solid-spheres applied. It is a function only of the droplet Reynolds number, Re_δ.

$$Re_\delta = \frac{V\, MVD\, \rho}{\mu} \tag{3}$$

Langmuir and Blodgett's tabulation of the range parameter was fit to the following expression for this study:

$$\frac{\lambda}{\lambda_{Stokes}} = \begin{pmatrix} 0.8388 + 0.001483\, Re_\delta \\ +0.1847\sqrt{Re_\delta} \end{pmatrix}^{-1} \tag{4}$$

Of more practical interest than K_0 is the collection efficiency at the leading edge, β_0, which was shown by Langmuir and Blodgett to be a function only of K_0,

$$\beta_0 = \frac{1.40\left(K_0 - \frac{1}{8}\right)^{.84}}{1 + 1.40\left(K_0 - \frac{1}{8}\right)^{.84}} \tag{5}$$

The accumulation parameter is:

$$A_c = \frac{LWC\, V\, \tau}{d\, \rho_i} \tag{6}$$

If all the water impinging on the leading edge freezes at that location and the leading-edge collection efficiency is 100%, A_c is a measure of the thickness of ice that will accrete relative to airfoil size.

The freezing fraction is the ratio of the amount of water entering a specified region on the surface that freezes there. From Messinger's[7] surface energy balance, the freezing fraction is

$$n = \frac{c_{p,ws}}{\Lambda_f}\left(\phi + \frac{\theta}{b}\right) \tag{7}$$

The individual terms in this expression are ϕ, the water energy transfer parameter,

$$\varphi = t_f - t_{st} - \frac{V^2}{2c_{p,ws}} \tag{8}$$

θ, the air energy transfer parameter,

$$\theta = \left(t_s - t_{st} - r\frac{V^2}{2c_p}\right) + \frac{h_G}{h_c}\left(\frac{\frac{p_{ww}}{T_{st}} - \frac{p_{tot}}{T_{tot}}\frac{p_w}{p_{st}}}{\frac{1}{.622}\frac{p_{tot}}{T_{tot}} - \frac{p_{ww}}{T_{st}}}\right)\Lambda_v \tag{9}$$

and b, the relative heat factor, introduced by Tribus, et. al.[8]

$$b = \frac{LWC\, V\, \beta_0\, c_{p,ws}}{h_c} \tag{10}$$

Equation (9) from Ruff includes compressibility effects. A simpler form without compressibility was used by Charpin and Fasso[9] and others. Ruff's expression for θ was used in this paper, but values found without compressibility are not significantly different for most icing conditions.

Rationale for Development of Additional Parameter

Because the Ruff method does not restrict the value of scale velocity, an additional similarity parameter can be used to determine V_S. Evidence that such a parameter was needed was provided by Bilanin and Anderson[2] in studies of the effect of changing surface tension of water. Figure 1 includes published and unpublished data from their studies and compares ice shapes with and without surfactant addition to the spray for velocities of 47, 67 and 94 m/s. The shaded ice shapes were obtained with the NASA Glenn Icing Research Tunnel (IRT) spray bar system de-mineralized water supply with no surfactant added, and the shape represented by the solid line resulted from surfactant addition to the water. Other than the addition of surfactant the same test conditions were used for each pair of tests, as shown in the accompanying table. Surfactant addition reduced the surface tension to roughly half that of water. Because n, β_0 and A_c were the same for each pair of tests, the leading-edge ice thickness was also nearly the same. However the included angle between the horns decreased dramatically when surfactant was added. Horn angle also decreased when velocity increased as can be seen by comparing figure 1(a) with (b) and (c). All the results shown were made at approximately the same freezing fraction. Thus, both surface tension and velocity have an effect on ice shape independent of freezing fraction, and scale velocity cannot be chosen arbitrarily. Clearly, then, a similarity parameter dependent on the ratio V^a/σ^b must be included in scaling methodology, where the powers a and b are not yet determined.

Additional evidence of the form of this parameter can

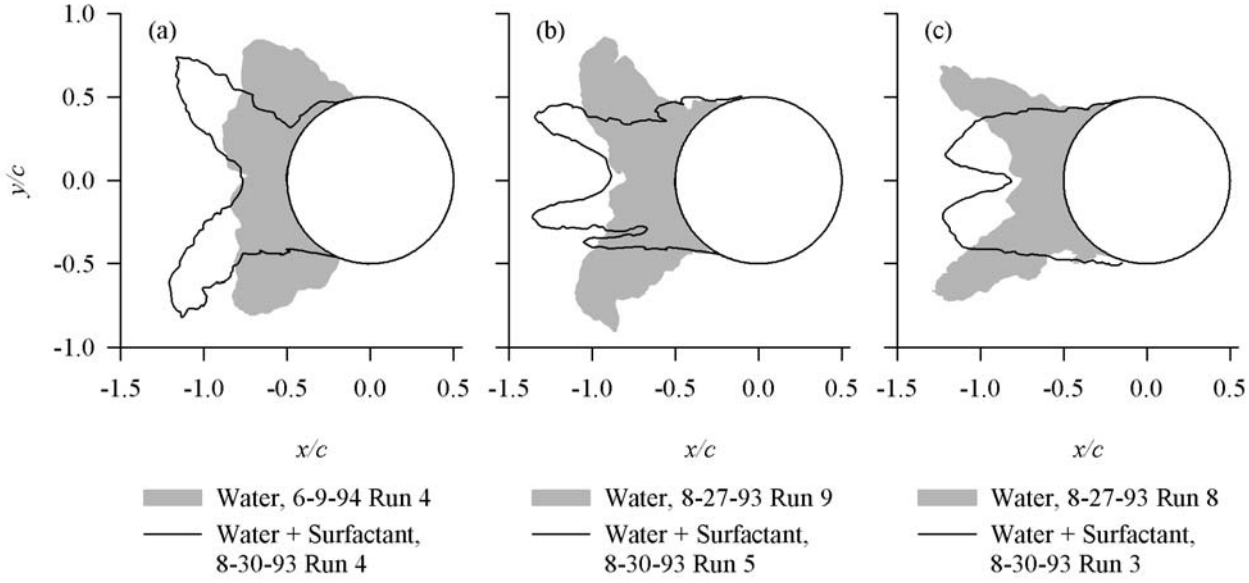

(a) V = 47 m/s (b) V = 67 m/s (c) V = 94 m/s

Date/Run	d, cm	t_{st}, °C	V, m/s	MVD, μm	LWC, g/m^3	τ, min	σ, dyne/cm	β_0, %	A_c	n	b	ϕ, °C	θ, °C	Re, 10^4	We, 10^3	We_c, 10^3	We_L, 10^6
(a) 6-9-94/4	5.1	-7.8	46.9	40.0	1.16	16.0	65	66.0	1.13	0.28	0.76	7.6	11.3	18.5	1.36	2.23	1.73
8-30-93/4	5.1	-8.0	46.8	40.0	1.17	16.0	30	66.0	1.13	0.29	0.76	7.7	11.5	18.5	2.91	4.80	3.71
(b) 8-27-	5.1	-11.8	66.9	34.1	1.39	10.2	65	65.4	1.22	0.33	1.08	11.3	15.7	26.7	2.35	4.53	3.51
8-30-93/5	5.1	-11.8	67.1	34.1	1.39	10.2	30	65.5	1.23	0.32	1.08	11.3	15.6	26.8	5.12	9.88	7.66
(c) 8-27-93/8	5.1	-12.2	94.0	30.0	1.10	9.0	65	65.6	1.20	0.31	1.03	11.2	14.0	36.6	4.08	8.7	6.94
8-30-93/3	5.1	-12.0	93.6	30.0	1.10	9.2	30	65.6	1.22	0.31	1.03	10.9	13.7	36.4	8.75	18.7	14.88

Figure 1. Effect of Surfactant and Velocity on Ice Shape. Vertical Cylinders Tested in the NASA Glenn IRT. Published and Unpublished Ice-Shape Data from Tests by Bilanin and Anderson.

be found from tests performed in the IRT in 1998 by Chen.[10] Chen studied a 61-cm-chord GLC 305 airfoil model in which only the droplet *MVD* was varied. Results for droplet sizes of 55 and 20μm at freezing fractions of 0.3 and 0.5 are given in figure 2. At each freezing fraction, the values of A_c, n, b, ϕ, θ and Re were maintained constant as drop size decreased. Although β_0 changed from about 92 to 74%, there was no measurable effect of reducing droplet size on the main ice shape. Undoubtedly, the icing limit would have changed with droplet size (that is, with β_0), but this feature was not measured. Chen's results, and others like them for NACA 0012 airfoils, show that the parameter being sought cannot be dependent on *MVD*. The present study included tests to evaluate if Chen's observations were also true for SLD conditions, and the results will be presented below.

Chen's investigation also included an evaluation of the effect of model size. Figure 3 illustrates that with β_0, A_c, n, b, ϕ and θ constant a reduction in chord from 91 to 30 cm moved the glaze horns rearward. This is the same effect shown in figure 1 for decreasing velocity.

Previous studies with both cylinders and NACA 0012 airfoils[11, 12] have shown that the temperature and *LWC* do not have effects on the ice shape independent of the freezing fraction. Thus, the general form of the supplementary parameter must be

$$P = \text{const}\,\frac{V^a c^c}{\sigma^b} \tag{11}$$

This form suggests a Weber number based on chord:

$$We_c = \frac{V^2 c \rho}{\sigma} \tag{12}$$

Studies by Bartlett[13, 14] and Oleskiw, et. al.[15] found no measurable effect of pressure on ice shape. These observations rule out the dependence on air density in equation (12), making water density a better choice. Furthermore, the length may not be chord itself but rather some physical characteristic related to the accreting ice that is proportional to chord; for example, the water-film thickness. Because this length is not yet identified, L will be used to represent it, and the Weber number is then

$$We_L = \frac{V^2 L \rho_w}{\sigma} \tag{13}$$

The trends apparent in figures 1 and 3 show that an increase in We_L has the same effect on glaze ice shape as an increase in n; that is, horns move back with an increase in the included horn angle as either n or We_L

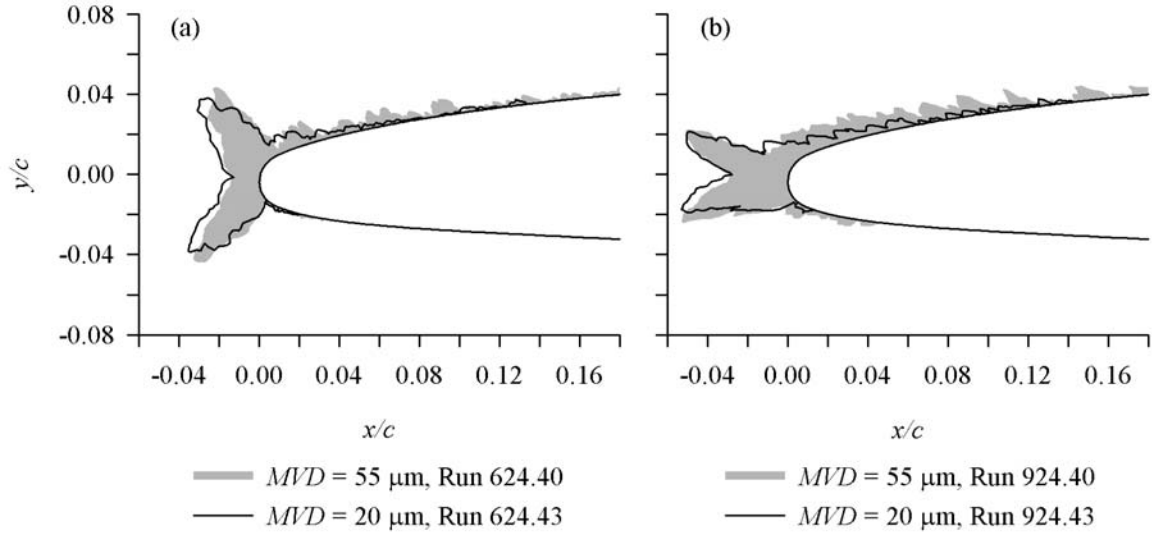

(a) $n = 0.28$ (b) $n = 0.52$

Run	c, cm	t_{st}, °C	V, m/s	MVD, μm	LWC, g/m^3	τ, min	β_0, %	A_c	n	b	ϕ, °C	θ, °C	Re, 10^4	We, 10^3	We_c, 10^3	We_L, 10^6
(a) 624.40	61.0	-10	90	55	1.16	6.1	91.6	2.53	0.28	0.84	8.9	11.3	10.9	6.76	2.49	2.02
624.43	61.0	-10	89	20	1.31	6.1	73.9	2.83	0.30	0.76	8.8	11.2	10.8	2.44	2.44	1.98
(b) 924.40	61.0	-17	90	55	1.16	6.1	91.7	2.53	0.51	0.84	15.9	20.5	11.4	6.77	2.56	2.02
924.43	61.0	-17	89	20	1.30	6.1	74.0	2.83	0.54	0.76	15.8	20.4	11.4	2.46	2.54	2.00

Figure 2. Effect of *MVD* on Ice Shape. GLC 305 Airfoil. Ice-Shape Data from Tests by Chen[10].

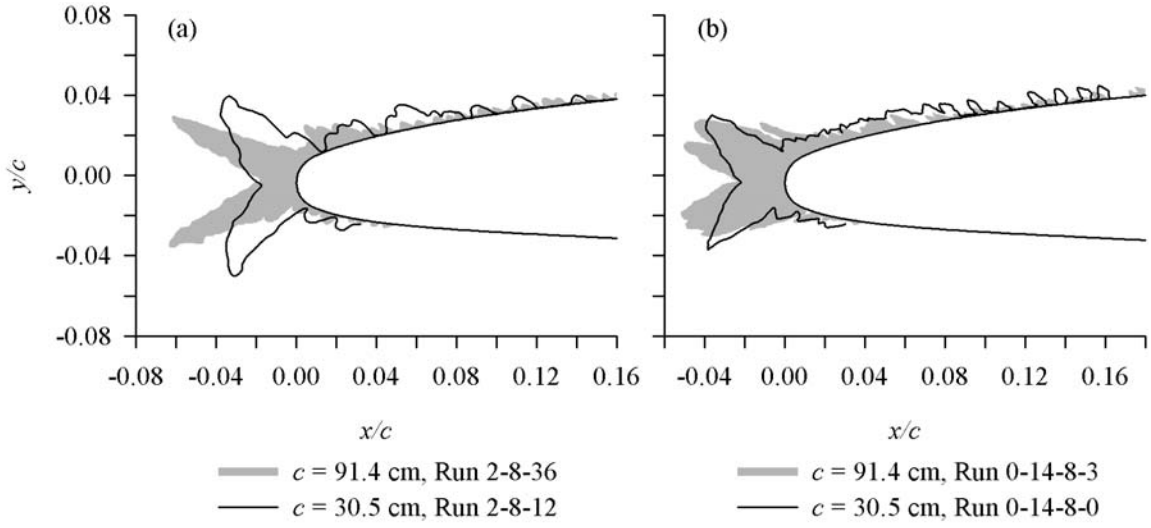

(a) $n = 0.4$ (b) $n = 0.5$

Run	c, cm	t_{st}, °C	V, m/s	MVD, μm	LWC, g/m^3	τ, min	β_0, %	A_c	n	b	ϕ, °C	θ, °C	Re, 10^4	We, 10^3	We_c, 10^3	We_L, 10^6
(a) 2-8-36	91.4	-12	118	44	0.58	14.6	87.2	2.67	0.40	0.57	10.8	11.8	21.4	9.54	6.41	5.28
2-8-12	30.5	-13	125	26	0.91	3.0	90.0	2.68	0.41	0.55	11.2	11.8	7.5	6.29	2.36	1.96
(b) 0-14-8-3	91.4	-15	121	38	0.55	13.5	84.9	2.40	0.52	0.54	13.3	14.8	22.2	8.59	6.76	5.54
0-14-8-0	30.5	-15	121	20	0.96	2.6	85.9	2.42	0.50	0.54	13.1	14.5	7.4	4.54	2.23	1.83

Figure 3. Effect of Model Size on Ice Shape. GLC 305 Airfoil. Ice-Shape Data from Tests by Chen.[10]

decrease. Weber numbers with other lengths have been considered in the past, such as one based on droplet size and water properties, *We*:

$$We = \frac{V^2 MVD \rho_w}{\sigma} \tag{14}$$

This Weber number seemed to be the logical choice based on the assumption that droplet splashing plays a role in establishing shapes for glaze ice. Anderson and Ruff[16], Anderson[17] and Kind[3] have all used the Weber number of equation (14). Because in most studies, the *MVD* was scaled along with chord, matching *We* would lead to scale velocities not too different from those obtained from matching We_L; thus, positive scaling results from these studies were probably misleading. Weber numbers based on various water film thickness expressions have also been evaluated[18,19] with encouraging outcomes, and it is possible that *L* will prove to be a water-film thickness.

With $L \propto d$ the scale velocity with $We_{L,S} = We_{L,R}$ is

$$V_S = V_R \sqrt{\frac{d_R}{d_S}} \tag{15}$$

where the subscripts *S* and *R* refer to scale and reference conditions, respectively. As a practical matter for tests with nearly constant air density, this result is little different from that obtained using constant We_c (eq. (12)). The present study will provide preliminary results to suggest that equation (13) provides an effective similarity parameter to supplement Ruff's basic scaling method for SLD reference conditions.

Test Description

The scaling tests were performed in the NASA Glenn IRT. The IRT is a closed-loop, refrigerated, sea-level tunnel with a rectangular test section measuring 1.8 by 2.7 m. It uses 10 spray bars to generate a cloud of supercooled droplets. The Appendix-C cloud calibration used for these tests was performed in the summer of 2000.[20]

The SLD calibration was made in the summer of 2002 using the same methods as the Appendix C. Only a few specific *MVD-LWC* combinations for speeds of 51, 77 and 103 m/s (100, 150 and 200 kt) have been calibrated to date. Therefore SLD tests are constrained to these particular conditions.

The models used were NACA 0012 airfoil sections with chords of 91.4, 53.3 and 26.7 cm. The 91.4-cm-chord airfoil is pictured in figure 4 (a). It was a full-span, fiberglass model and served as the reference model. The 53.3-cm-chord model (1.7:1 scale) was of 61-cm

(a) 91.4-cm-Chord NACA 0012 Model Installed in IRT Test Section.

(b) 53.3-cm-Chord NACA 0012 Model Installed in IRT Test Section.

Figure 4. Model Description.

span and made of aluminum. It was mounted vertically between splitter plates at the center of the IRT test section as shown in figure 4(b). Horizontal lines at the leading edge indicated tunnel center, ±2.5 cm and ±5 cm from the center as guides for locating ice tracings. The 26.7-cm model (3.4:1 scale) was also of 61-cm span. Its appearance and mounting method were similar to the 53.3-cm. All tests were run at 0° AOA although the mounting arrangement permitted rotation of the model for angle of attack changes.

The IRT spray system has the ability to produce a stabilized spray within a few seconds of start; thus, shielding of the models was not needed during spray initiation.

In preparing for a test, the temperature and airspeed in the test section and the air and water pressures on the spray manifolds were set. When these conditions had stabilized, the spray nozzle valves were opened to initiate the spray. The spray was timed for the required duration, and then turned off. The fan was brought to a full stop and the tunnel entered to record the ice shape. A heated ice knife with a cutout in the shape of the model was inserted into the leading edge of the ice to melt a thin slice down to the model surface. A cardboard template was placed into this gap and an outline of the ice accretion traced. Tracings were taken at the vertical center of the tunnel (91 cm from the floor) and at 2.5 cm above the center. Ice shape differences between the two tracing locations were never significant and only centerline shapes will be reported here. The tracings were digitized and the *x*-*y* coordinates for each ice shape recorded. The coordinates have been normalized by the model chord for presentation here.

Uncertainty Analysis

Uncertainties in the test conditions were estimated from differences between individual instrument readings, instrument uncertainty and fluctuations over the spray duration. Temperatures were believed to be good to ±0.5°C, and the uncertainty in velocity was estimated to be 3%. For Appendix-C conditions the net uncertainty in *MVD* was estimated at ±12%. For SLD conditions it may have been as much as ±25%. These uncertainties are not referenced to an absolute value of *MVD*, which is unknown. Repeatability and scatter in the *LWC* calibration data suggests the uncertainty is about ±10% for both Appendix-C and SLD conditions.

These uncertainties in the test parameters were estimated to produce the following uncertainties in the similarity parameters for the Appendix-C tests: 8% in β_0, 10% in A_c, 15% in n, 2% in Re, 13% in We and 5% in We_L. For the SLD tests the uncertainties were: 4% in β_0, 10% in A_c, 15% in n, 2% in Re, 26% in We and 5% in We_L.

Results

The effect of droplet size is shown in figure 5, which compares ice shapes obtained for SLD droplet sizes

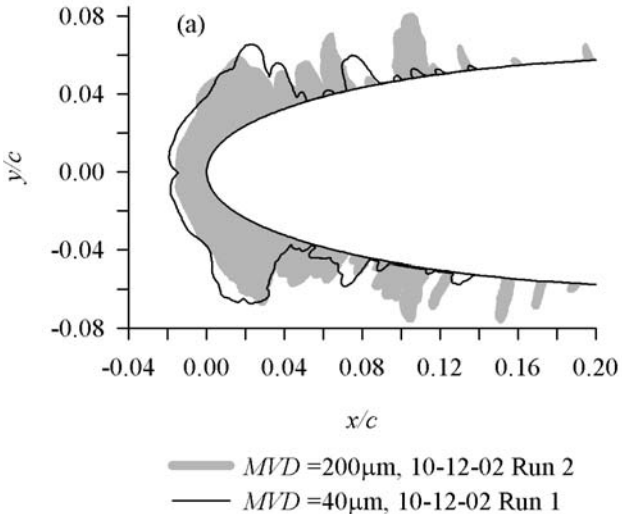

(a) *MVD*, 200 and 40μm; *c*, 53.3 cm; *V*, 51 m/s; *n*, 0.3.

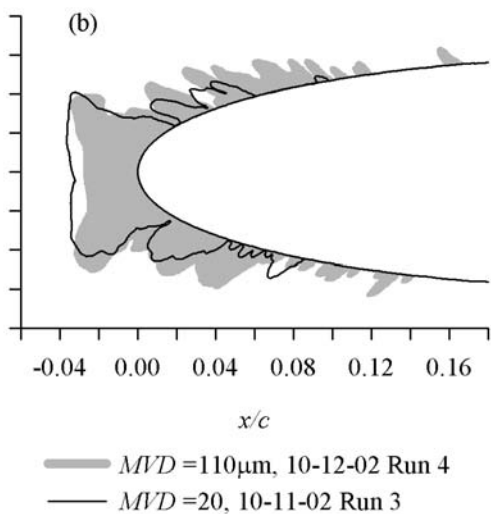

(b) *MVD*, 110 and 20μm; *c*, 53.3 cm; *V*, 51 m/s; *n*, 0.5.

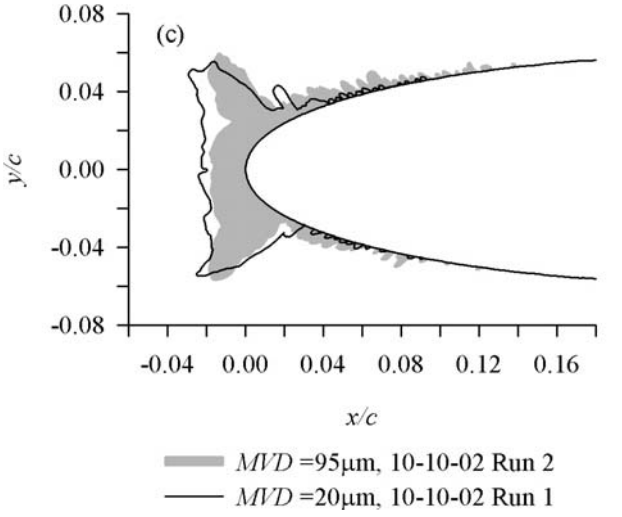

(c) *MVD*, 95 and 20μm; *c*, 91.4 cm; *V*, 77 m/s; *n*, 0.3

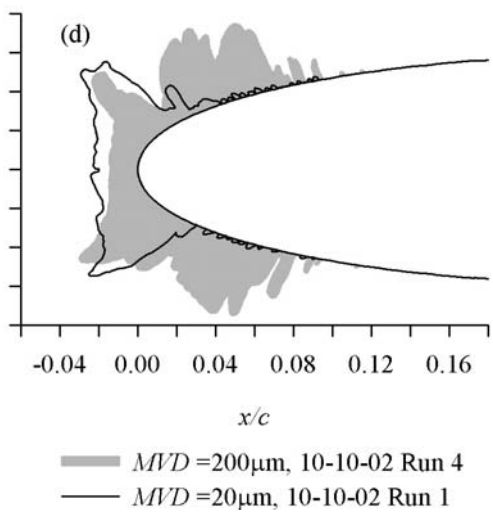

(d) *MVD*, 200 and 20μm; *c*, 91.4 cm; *V*, 77 m/s; *n*, 0.3

Date/Run	c, cm	t_{st}, °C	V, m/s	MVD, μm	LWC, g/m^3	τ, min	β_0, %	A_c	n	b	ϕ, °C	θ, °C	Re, 10^4	We, 10^3	We_c, 10^3	We_L, 10^6
(a) 10-12-02/2	53.3	-8	51	200	1.20	7.1	97.8	1.71	0.32	0.70	8.1	11.9	6.7	8.13	0.88	0.69
10-12-02/1	53.3	-6	51	40	1.13	10.8	84.0	2.44	0.28	0.57	6.1	9.0	6.6	1.62	0.87	0.68
(b) 10-12-02/4	53.3	-11	51	120	1.03	9.4	95.7	1.92	0.49	0.59	11.2	16.2	6.8	4.80	0.88	0.68

with those at Appendix-C conditions. Recorded test conditions and corresponding similarity parameters for each of the tests are given in a table accompanying the figure. Tests were run using the same NACA 0012 model at the same velocity for each pair of shapes. Temperatures were determined to provide a match of the freezing fraction for each pair. The stagnation-line collection efficiency, β_0, could not be matched, but conditions were chosen so that the product of $\beta_0 A_c$ would match. Later evaluation of calibration data indicated that the actual $\beta_0 A_c$ for each pair of shapes probably differed by 12 – 22%. This disagreement explains the differences observed in the leading-edge ice thickness for each pair of shapes.

For figure 5(a), ice shapes obtained with 200 and 40μm are compared for the 53-cm model at 51 m/s. For 5(b) 110 and 20μm are compared for the same model and velocity as for 5(a). Figures 5(c) and (d) show ice shapes recorded at 77 m/s for the 91-cm model. 5(c) compares a 95-μm *MVD* shape with that of 20-μm, and (d) a 200-μm and 20-μm. For each of the comparisons, the main ice shape was little changed by the reduction in *MVD* from SLD conditions to an Appendix-C value.

This correspondence of the main ice shape over wide ranges of drop size indicates that it should be relatively easy to simulate SLD conditions with Appendix-C droplet sizes, at least for the conditions studied here, if the main ice shape is of primary interest. However, two other features of those SLD accretions need to be noted. First, when drop sizes were larger than about 100μm the feather structures aft of the main ice shape were significantly larger than those of the Appendix-C shapes. These large feathers were particularly prominent for an *MVD* of 200μm. Further study is needed to determine under what conditions these growths occur, the physics behind them and whether they can be simulated in small-droplet accretions.

Second, because the SLD collection efficiency was so much larger than that for Appendix-C conditions the SLD accretions featured small feathers well aft of the Appendix-C icing limits. Figure 6 gives recorded icing limits, normalized with respect to chord, for both the 91- (solid symbols) and 53-cm models (open symbols) including all the Appendix-C and SLD test conditions for this study. These limits were recorded at the completion of each test at the same time the ice was traced. Each data point represents the average of 4 estimates: the upper and lower surface limits for each of two ice tracing locations. Near the aft extent of icing, feathers become small and sparsely distributed. Therefore, significant variability in the estimated limit from run to run was experienced. The large scatter within the data for each model size was indicative of

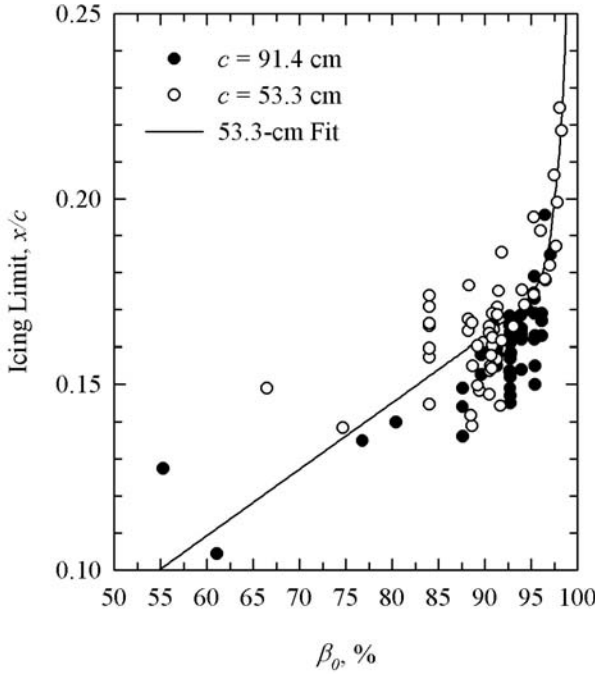

Figure 6. Icing Limits for Two NACA 0012 Models.

for each model size was indicative of this variability. The results were estimated to have an uncertainty of about ±20%.

The icing limits in figure 6 correlate with β_0 although the bulk of the data with the larger model tend to fall below those from the smaller model. A fit of the 53-cm data is shown with a solid line which passes through the origin. No correlation with test parameters was observed, indicating that it should be possible to determine icing limits for SLD conditions from tests at Appendix-C conditions if β_0 is matched. For scale tests it is always desirable to match β_0 to the reference value. However, if this cannot be done for the desired conditions, the main ice shape and icing limit can be determined with separate tests: one with unmatched β_0 to find the main ice shape and one to determine the effect of β_0 on icing limit.

The results of figure 5 confirm Chen's observations that main ice shapes are not affected by *MVD*. Thus, even for SLD conditions the We_L of equation (13) is a more likely form of Weber number than the *We* of equation (14). To test the validity of finding scale velocity by matching scale and reference We_L, SLD ice shapes were compared with those from Appendix-C conditions for which We_L matched. The results are given in figure 7. Reference ice shapes were obtained with a 91-cm-chord 0012 model and an *MVD* of 160 μm. The velocity was 51 m/s, *LWC* was 1.50 g/m^3 and the spray time 9.7 min.

Static temperature was varied from -11 to -19°C to give nominal freezing fractions of 0.3, 0.4 and 0.5. These freezing fractions were chosen to match values for previous Appendix-C tests using 53.3- and 26.7-cm-

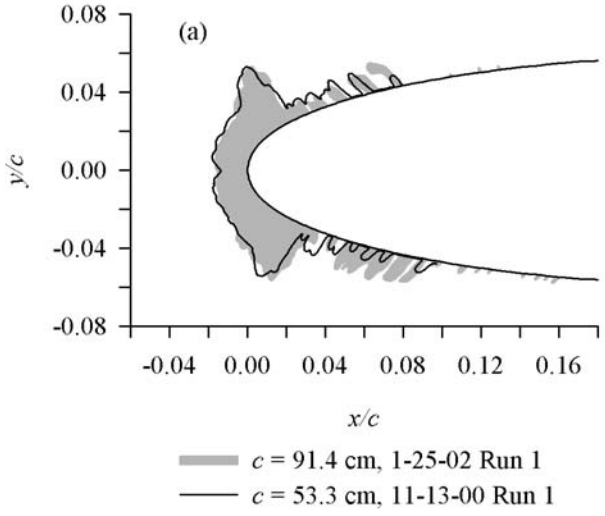

(a) Model Chord Scaled from 91 to 53 cm; *n*, 0.3.

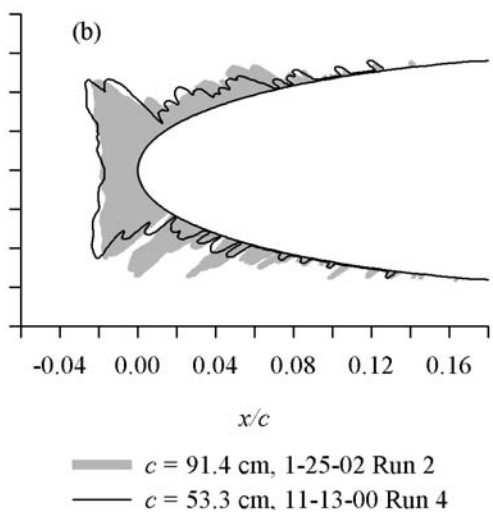

(b) Model Chord Scaled from 91 to 53 cm; *n*, 0.4.

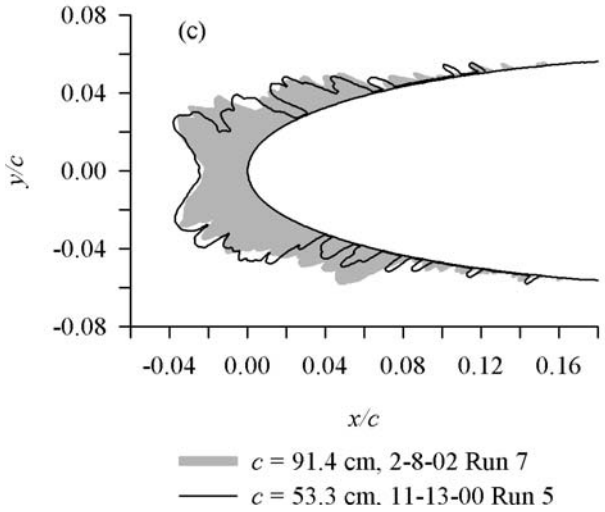

(c) Model Chord Scaled from 91 to 53 cm; *n*, 0.5.

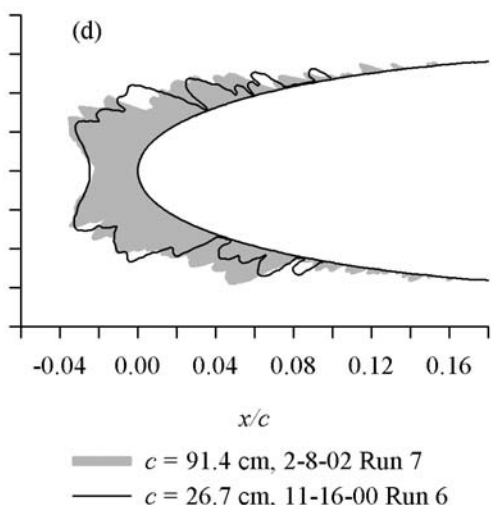

(d) Model Chord Scaled from 91 to 27 cm; *n*, 0.5.

Date/Run	c, cm	t_{st}, °C	V, m/s	MVD, μm	LWC, g/m^3	τ, min	β_0, %	A_c	n	b	ϕ, °C	θ, °C	Re, 10^4	We, 10^3	We_c, 10^3	We_L, 10^6
(a) 1-25-02/1	91.4	-11	51	160	1.50	9.7	95.4	1.70	0.30	1.26	11.1	16.0	11.6	6.50	1.52	1.17
11-13-00/1	53.3	-7	67	38	1.00	7.3	84.9	1.88	0.28	0.58	6.6	9.0	8.6	2.61	1.47	1.15
(b) 1-25-02/2	91.4	-15	51	160	1.50	9.7	95.4	1.70	0.40	1.26	14.9	21.1	12.0	6.50	1.55	1.17
11-13-00/4	53.3	-10	67	38	1.00	7.3	84.9	1.88	0.40	0.58	9.2	12.9	8.7	2.60	1.48	1.15
(c) 2-8-02/7	91.4	-19	52	160	1.50	9.7	95.4	1.70	0.50	1.25	18.9	25.9	12.4	6.54	1.58	1.18
11-13-00/5	53.3	-13	67	38	0.99	7.3	84.9	1.88	0.52	0.58	12.0	16.6	8.9	2.62	1.51	1.16
(d) 2-8-02/7	91.4	-19	52	160	1.50	9.7	95.4	1.70	0.50	1.25	18.9	25.9	12.4	6.54	1.58	1.18
11-16-00/6	26.7	-14	110	21	0.91	2.4	85.8	1.88	0.52	0.49	12.2	14.2	7.0	3.96	1.95	1.57

Figure 7. Ice-Shape Comparisons for Constant or Nearly Constant We_L.

chord NACA 0012 models.[19] These Appendix-C ice shapes will serve as scale results for the present study. While it was not possible to match reference and scale β_0, the values were within 12%, which as shown above is more than adequate for scaling main ice shapes. What is more important, the product $\beta_0 A_c$ matched for each pair of tests compared. Values of b, ϕ and θ did not match. Conditions for the 53.3-cm model tests were such that We_L matched that of the 91.4-cm, while We_L for the 26.7-cm tests was about 30% higher than the reference for the example shown. The 26.7-cm-chord scale conditions providing an exact match of the reference We_L will be tested in a future study.

In figure 7 the shaded ice shape is that obtained with the 91.4-cm-chord at SLD conditions. The solid line shows the Appendix-C (scale) shape. Test conditions and corresponding similarity parameters for each set of tests are given in the table accompanying the figure.

Figure 7(a) shows the ice shapes for a freezing fraction of 0.3. The 53.3-cm-chord 38-μm-*MVD* test produced a main ice shape in very close agreement with the 91.4-cm-chord 160-μm-*MVD* shape. In addition, the sizes of both the large feathers adjacent to the main shape and the smaller feathers further aft were simulated well.

Figure 7(b) compares the 91.4-cm reference with the 53.3-cm-chord scale result for a freezing fraction of 0.4. The 53.3-cm-chord Appendix-C ice shape again gave an excellent match of the 91.4-cm-chord SLD shape, although the lower-surface feathers just aft of the main shape were significantly larger for the SLD conditions.

Figures 7(c) and (d) give results for a freezing fraction of 0.5 with the 91.4-cm reference conditions scaled to 53.3 and 26.7 cm, respectively. Scale and reference ice shapes were in very good agreement for both scale models. The scale ice shapes for the 26.7-cm model matched the SLD reference for the freezing fractions of 0.3 and 0.4, as well, showing that SLD ice shapes can be simulated at scale ratios of at least 3.4:1.

Other Appendix-C tests with the 26.7-cm chord model were performed with different velocities than that shown in figure 7(d). None of these exactly matched the value satisfying constant We_L; however, the best match of the SLD shapes occurred when velocities close to the value required to match We_L were selected.

Appendix-C tests with these same conditions have been repeated in several other tunnel entries over the last 2 years. Because ice shapes vary somewhat from one entry to another, agreement of Appendix-C and SLD results for other entries was not always as good as shown here.

The generally good agreement of ice shapes in this study suggests that the parameters b, ϕ and θ, scale values of which did not match the reference, can be ignored as long as the freezing fraction matches.

Concluding Remarks

Ice-shape evidence showed that an important similarity parameter needed in scaling analyses is the Weber number based on a length, L, proportional to model size. Thus,

$$We_L = \frac{V^2 L \rho_w}{\sigma} \tag{16}$$

Good scaling was achieved in this study by matching scale and reference values of the parameters n and We_L and the product $\beta_0 A_c$. Scale size ratios were as large as 3.4:1 and freezing fractions covered the range from 0.3 to 0.5.

Good agreement of both quantity and shape of the main ice accumulation between Appendix-C scale conditions and 160-μm SLD reference conditions was observed. Tests that directly compared ice shapes formed at 200μm and at 20μm also showed good agreement of the main accretions. These results argue against a significant role of splashing for the SLD conditions considered. However, the mechanism of formation of large feather structures seen in SLD accretions for *MVD*'s larger than about 100μm needs to be researched. The present SLD reference tests were made with velocities of about 50 and 77 m/s, and these conclusions may not be valid for higher velocities.

Additional analysis is needed to identify the appropriate length L for use in the Weber number of equation (16). The ice shapes analyzed and compared in this study suggest that L is either independent of *MVD* and *LWC*, or only weakly dependent, while it is proportional to model size.

This and other scaling studies have shown that *LWC* can be chosen fairly arbitrarily as long as reference and scale freezing fractions match. Excellent scaling results were obtained in this study without matching b, ϕ, or θ. It should be possible to gain flexibility in scaling tests, then, by choosing convenient values for *LWC* and temperature with the only constraint being that the freezing fraction matches the reference value. It was also shown that, while it is desirable to match β_0, main ice shapes appear to be independent of *MVD*. The ability to set scale *MVD* to values convenient to the test facility adds additional flexibility in determining scale conditions. The main effect of *MVD* (through β_0) is on the icing limit, but because icing limits can be correlated with β_0, tests of scale-model icing limit for a range of β_0 can be

run independently of those recording the main ice shape. This approach should provide adequate information about that characteristic.

References

[1] Ruff, G.A., "Analysis and Verification of the Icing Scaling Equations," AEDC-TR-85-30, vol 1 (rev), March 1986.

[2] Bilanin, Alan J. and Anderson, David N., "Ice Accretion with Varying Surface Tension," AIAA-95-0538 and NASA TM 106826, January 1995.

[3] Kind, R.J., Dillon, T., Gaydos, J.A. and Oleskiw, M., "Evidence for the Importance of Scaling Viscous Effects in the Water Film in Glaze Icing Tests," AIAA-98-0196, January 1998.

[4] Feo, A., "Icing Scaling with Surface Film Thickness Similarity for High *LWC* Conditi ons," AE/PRO/4420/184/INTA/00, Instituto Nacional de Técnica Aeroespacial, October 2000.

[5] Langmuir, Irving and Blodgett, Katharine B.: "A Mathematical Investigation of Water Droplet Trajectories," Army Air Forces Technical Report No. 5418, February 1946.

[6] Abbott, Ira H. and von Doenhoff, Albert E., *Theory of Wing Sections*, Dover, New York, 1959, pp114 and 321.

[7] Messinger, B.L., "Equilibrium Temperture of an Unheated Icing Surface as a Function of Airspeed," *J. Aeron. Sci.*, vol. 20 no. 1, January 1953, pp 29 – 42.

[8] Tribus, Myron, Young, G.B.W. and Boelter, L.M.K., "Analysis of Heat Transfer Over a Small Cylinder in Icing Conditions on Mount Washington," *Trans. ASME*, vol. 70, November 1948, pp 971 – 976.

[9] Charpin, Francois and Fasso, Guy, "Essais de givrage dans la grande soufflerie de Modane sur maquettes a echelle grandeur et echelle reduite," *L'Aeronautique et l'Astronautique*, no. 38, 1972, pp 23 – 31. English translation published as "Icing Testing in the Large Modane Wind-Tunnel on Full-Scale and Reduced Scale Models," NASA TM-75373, March 1979.

[10] Chen, Shu-Cheng, unpublished GLC 305 icing studies in NASA Glenn IRT, March, April, September and October 1998.

[11] Anderson, David N., "Methods for Scaling Icing Test Conditions," AIAA-95-0540, January 1995.

[12] Anderson, David N., "Further Evaluation of Traditional Icing Scaling Methods," AIAA-96-0633, January 1996.

[13] Bartlett, C. Scott, "An Analytical Study of Icing Similitude for Aircraft Engine Testing," DOT/FAA/CT-86/35 and AEDC-TR-86-26, October 1986.

[14] Bartlett, C. Scott, "Icing Scaling Considerations for Aircraft Engine Testing," AIAA-88-0202, January 1988.

[15] Oleskiw, Myron M., De Gregorio, Fabrizio and Esposito, Biagio, "The Effect of Altitude on Icing Tunnel Airfoil Icing Simulation," *Proceedings of the FAA International Conference on Aircraft Inflight Icing*, DOT/FAA/AR-96/81,II, August 1996, pp 511 – 520.

[16] Anderson, David N. and Ruff, Gary A., "Evaluation of Methods to Select Scale Velocities in Icing Scaling Tests," AIAA-99-0244, January 1999.

[17] Anderson, David N., "Effect of Velocity in Icing Scaling Tests," AIAA-2000-0236, January 2000.

[18] Kind, Richard J., "Assessment of Importance of Water-Film Parameters for Scaling of Glaze Icing," AIAA-2001-0835, January 2001.

[19] Anderson, David N. and Feo, Alejandro, "Ice-Accretion Scaling Using water-Film Thickness Parameters," AIAA-2002-0522, January 2002.

[20] Ide, Robert F. and Oldenburg, John R., "Icing Cloud Calibration of the NASA Glenn Icing Research Tunnel," AIAA-2001-0234, January 2001.

REPORT DOCUMENTATION PAGE

Form Approved
OMB No. 0704-0188

1. AGENCY USE ONLY (*Leave blank*)	2. REPORT DATE	3. REPORT TYPE AND DATES COVERED
	August 2005	Final Contractor Report

4. TITLE AND SUBTITLE

Additional Results of Ice-Accretion Scaling at SLD Conditions

5. FUNDING NUMBERS

WBS–22–728–41–17
NCC3–884

6. AUTHOR(S)

David N. Anderson and Jen-Ching Tsao

7. PERFORMING ORGANIZATION NAME(S) AND ADDRESS(ES)

Ohio Aerospace Institute
22800 Cedar Point Road
Brook Park, Ohio 44142

8. PERFORMING ORGANIZATION REPORT NUMBER

E–15220

9. SPONSORING/MONITORING AGENCY NAME(S) AND ADDRESS(ES)

National Aeronautics and Space Administration
Washington, DC 20546–0001

10. SPONSORING/MONITORING AGENCY REPORT NUMBER

NASA CR—2005–213850
AIAA–2003–0390

11. SUPPLEMENTARY NOTES

Prepared for the 41st Aerospace Sciences Meeting and Exhibit sponsored by the American Institute of Aeronautics and Astronautics, Reno, Nevada, January 6–9, 2003. Project Manager, Thomas H. Bond, Instrumentation and Controls Division, NASA Glenn Research Center, organization code RI, 216–433–3900.

12a. DISTRIBUTION/AVAILABILITY STATEMENT

Unclassified - Unlimited
Subject Category: 03

Available electronically at http://gltrs.grc.nasa.gov

This publication is available from the NASA Center for AeroSpace Information, 301–621–0390.

12b. DISTRIBUTION CODE

13. ABSTRACT ***(Maximum 200 words)***

To determine scale velocity an additional similarity parameter is needed to supplement the Ruff scaling method. A Weber number based on water droplet MVD has been included in several studies because the effect of droplet splashing on ice accretion was believed to be important, particularly for SLD conditions. In the present study, ice shapes recorded at Appendix-C conditions and recent results at SLD conditions are reviewed to show that droplet diameter cannot be important to main ice shape, and for low airspeeds splashing does not appear to affect SLD ice shapes. Evidence is presented to show that while a supplementary similarity parameter probably has the form of a Weber number, it must be based on a length proportional to model size rather than MVD. Scaling comparisons were made between SLD reference conditions and Appendix-C scale conditions using this Weber number. Scale-to-reference model size ratios were 1:1.7 and 1:3.4. The reference tests used a 91-cm-chord NACA 0012 model with a velocity of approximately 50 m/s and an MVD of 160μm. Freezing fractions of 0.3, 0.4, and 0.5 were included in the study.

14. SUBJECT TERMS

Icing physics; Scaling; SLD; LWC

15. NUMBER OF PAGES

17

16. PRICE CODE

17. SECURITY CLASSIFICATION OF REPORT	18. SECURITY CLASSIFICATION OF THIS PAGE	19. SECURITY CLASSIFICATION OF ABSTRACT	20. LIMITATION OF ABSTRACT
Unclassified	Unclassified	Unclassified	